ELSEVIER

Catalysis Today 59 (2000) 131–140

CATALYSIS TODAY

www.elsevier.com/locate/cattod

Experimental and numerical investigation on the influence of temporal fuel/air unmixedness on NO_x emissions of lean premixed catalytically stabilized and non-catalytic combustion

A.L. Boehman [a,*], R.W. Dibble [b,1]

[a] *Department of Energy and Geo-Environmental Engineering, The Pennsylvania State University, 114B Hosler Building, University Park, PA 16802-5000, USA*

[b] *Department of Mechanical Engineering, 6159 Etcheverry Hall, University of California, Berkeley, CA 94720-1740, USA*

Abstract

The influence of temporal fuel/air unmixedness on NO_x emissions in lean premixed catalytically stabilized and non-catalytic combustion of propane is experimentally and numerically investigated. Experiments are performed in a tubular, adiabatic flow reactor with catalytically active and inactive honeycomb structures inserted at the inlet to the combustion chamber. Catalytically stabilized combustion is performed as "hybrid" catalytic combustion, where only a fraction of the fuel is consumed within the catalyst and the remaining fuel is burned downstream in a homogeneous combustion zone. A special mixing section is used which allows variation of frequency and magnitude of temporal fuel fluctuations while maintaining spatially uniform conditions over the cross-section. Numerical investigations are performed by coupling a transient catalyst model with a PFR model for hybrid catalytic combustion and a PFR model for non-catalytic combustion. The catalyst model comprises a 2D model for the gas phase and a 1D model for the catalyst substrate, including one-step surface kinetics for propane oxidation. The PFR model uses a detailed reaction mechanism to model NO_x formation in the homogeneous combustion zone.

It is shown experimentally that NO_x emissions from catalytically stabilized combustion are much less sensitive to temporal fuel/air unmixedness than non-catalytic combustion. The catalyst model reveals (1) that the catalyst lowers the mean fuel concentration and the magnitude of the fluctuations prior to the homogeneous combustion zone downstream of the catalyst and (2) that the catalyst's thermal inertia acts as a buffer for the fluctuating heat release on the surface, i.e., it prevents the development of large temperature fluctuations in the gas phase. Comparison of modeled NO_x emissions with experimental data shows good agreement for non-catalytic combustion, but poor agreement for hybrid combustion. These findings are discussed in detail and improvements are suggested to improve agreement between experiment and prediction for the hybrid combustion case.

Keywords: NO_x; Catalytic combustion; Lean premixed

1. Introduction

Lean premixed combustion is one of the most successful techniques for achieving very low NO_x emissions from gas turbine combustion chambers. However, recent studies have shown that the fuel/air mixing quality prior to the combustion process has a

* Corresponding author. Tel.: +1-814-865-7839.
E-mail addresses: boehman@ems.psu.edu (A.L. Boehman), rdibble@newton.me.berkeley.edu (R.W. Dibble)
[1] Tel.: +1-510-642-4901.

0920-5861/00/$ – see front matter
PII: S0920-5861(00)00278-9

great influence on NO_x emissions [1–3]. It is widely recognized that combustion under perfectly premixed conditions results in the lowest achievable NO_x emissions. Any incomplete premixing of fuel and air will increase emissions. Incomplete premixing means that pockets which are leaner and richer than the mean fuel concentration are burnt in the combustion process, leading to lower and higher temperatures than the mean combustion temperature. As NO_x formation in the lean regime is a non-linear, highly temperature dependent process, the overall NO_x formation is increased.

Incomplete premixing or "unmixedness" of fuel and air can occur as spatial and/or temporal unmixedness. There is no principal difference between these two forms of unmixedness, since temporal fluctuations are simply spatial unmixedness in the direction of flow. However, temporal unmixedness cannot be detected with conventional suction probe analyzers since their time resolution is normally too low.

Recent studies have shown, that although spatial uniformity in fuel concentration may be achieved in the premixing section, "hidden" temporal concentration fluctuations strongly increase NO_x emissions [1,4]. Hidden in this context means that these fluctuations could not be resolved by the conventional analyzers used. Since it is very costly to achieve perfect temporal mixing in technical applications, the lowest theoretically possible NO_x emissions for perfectly premixed, lean combustion are rarely being reached.

Catalytically stabilized combustion has been proposed as a way to improve lean stability and to achieve low NO_x emissions [5]. Due to temperature limitations of materials and the steady increase in gas turbine inlet temperatures, "hybrid" designs have to be applied, where the catalyst is kept at a lower temperature than the overall flame temperature. This can be achieved by converting only a certain fraction of the fuel within the catalyst while combustion is completed in a homogeneous combustion zone downstream of the catalyst [6–10].

The requirements on the mixing quality for catalytic combustion are somewhat different than for non-catalytic combustion. Spatially uniform inlet conditions are important as well, but not only to avoid increased NO_x formation, but also to remain well within the operating window of a certain catalyst design [8]. On the other hand, the requirements on temporal premixing are less stringent. In a recent study [4], it was shown experimentally that increase of NO_x emissions as a result of temporal fuel fluctuations are much smaller with catalytically stabilized combustion than with non-catalytic combustion.

Although experimentally evident, the catalyst's large impact to reduce the overall NO_x emissions due to temporal fuel/air unmixedness is not yet fully understood. This paper briefly reviews experimental data on the influence of temporal fuel fluctuations on NO_x emissions from both catalytically stabilized and non-catalytic, lean premixed combustion. The main focus, however, is to describe the modeling approach for a hybrid catalytic combustor and to compare its numerical results on NO_x emissions with experimental data.

2. Experimental

A brief description of the experimental set-up, the diagnostic tools and the experimental conditions is given here. More details can be found in [4]. Fig. 1 shows a schematic of the test rig which consists of a

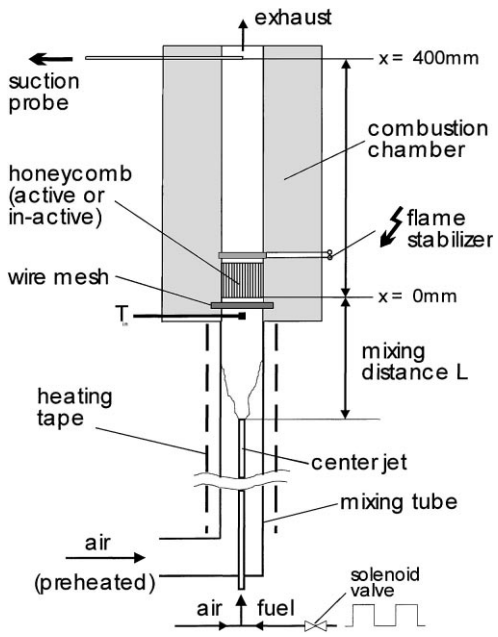

Fig. 1. Schematic of the test rig with mixing section and combustion chamber.

mixing section and a combustion chamber. The mixing section is designed to achieve the following inlet conditions: (1) plug flow profiles of temperature and velocity are constant over time, (2) plug flow profiles of fuel concentration at any time but temporally fluctuating. The temporal fluctuations can be varied in magnitude and frequency.

Air is electrically preheated and fed into a 1 m mixing tube (i.d. 26.4 mm) to act as coflow. The tube is wrapped with heating tape maintained at the inlet temperature to the combustion chamber, T_{in}, to prevent the development of radial temperature profiles. Several layers of fine wire mesh are located at the exit of the mixing section (the inlet to the combustion chamber) to guarantee a uniform velocity profile over the cross-section. Upstream radiation from the combustion chamber is absorbed by the mesh and uniformly transferred to the fuel/air mixture, generating adiabatic conditions in terms of radiation.

Propane and a small part of the total air are injected via a center jet tube (i.d. 1.4 mm). The additional air enhances turbulent mixing with the coflow. The fuel flow can be pulsed in different frequencies by a solenoid valve (on/off mode) and the magnitude of the fuel fluctuations can be varied by varying the mixing distance L. As is shown in [4], a wide range of "rms fluctuations in fuel concentration" could be achieved by choosing frequencies of 10, 20 and 30 Hz and varying the mixing distance from 28.5 to 98.5 cm. Temporal fluctuations of fuel concentrations matched very closely a sine-wave in function of time. In practical applications, higher frequencies can also be observed, but this experimental range was purposely chosen, since lower frequencies are expected to have a greater impact on the catalyst performance.

The combustion chamber is an insulated, tubular reactor (i.d. 25.4 mm). Honeycomb monoliths of 20 mm length with 1.5 mm square cells are placed at the inlet of the combustion chamber. These monoliths (cordierite) are either inactive for non-catalytic combustion or coated with Pt on Al_2O_3 washcoat for catalytically stabilized combustion. In order to stabilize the homogeneous combustion at a fixed location and therefore to achieve a defined residence time in all cases, a thin, electrically heated SiC filament is placed immediately downstream of the monolith. The additional energy input into the gas stream by this flame stabilizer is small compared to the chemical heat released by the fuel oxidation (<1%), thereby minimizing the effect on NO_x emissions. However, the electric power supplied is monitored and kept constant in all cases.

Measurements of temporal fuel concentration are performed by absorption of laser light at 3.39 μm (He–Ne laser) at the inlet plane to the combustion chamber (x=0 mm). The data obtained with this method are expressed as rms fluctuations of fuel concentration, which is defined as $F = c'_{rms}/\bar{c}$. Species measurements such as CO, CO_2, O_2, UHC, NO/NO_x are made with "conventional" suction probe analyzers on a dry basis and a suction probe placed at the exit of the combustion chamber (x=400 mm). More details about the diagnostic tools can be found in [4].

The experimental conditions used in this paper are: atmospheric pressure, inlet temperature T_{in}=400°C, coflow air flow=96 standard liters per minute (SLM), jet air flow=4 SLM and jet propane flow=2.1 SLM. Throughout the measurements, all flows are kept constant yielding an overall equivalence ratio ϕ equal to 0.5.

3. Modeling

It has been demonstrated in earlier studies [10,11], that NO_x emissions emerging from a hybrid catalytic combustor can be modeled as a combination of a catalyst model and a plug flow reactor (PFR), where the PFR describes the homogeneous combustion zone downstream of the catalyst. For this investigation a catalyst model has been developed which includes certain transient terms to account for temporal fluctuations of the inlet conditions.

3.1. Catalyst model

The catalyst model considers a single adiabatic cell within the monolith and consists of: (1) a 2D solution of the cylindrical axisymmetric momentum, heat and mass transport equations; and (2) a 1D energy balance for the cell wall. The numerical model simulates a developing 2D laminar flow and calculates axial surface temperature profiles. The rectangular monolith cell is approximated as a cylinder of equal hydraulic diameter. The model accommodates transient inlet conditions to simulate the temporal fuel/air unmixedness,

and is based on a previous model that considered transient thermal stress formation within ceramic catalytic combustors [12,13].

The governing equations for a transient 2D model of a catalytic passage include a set of convection/diffusion equations for momentum, energy and species in the gas stream, and an energy balance for the catalytic surface. Surface diffusion of species is built into the reaction rate law for heterogeneous chemistry [14]. Local transport and thermodynamic properties are evaluated with the CHEMKIN library package [15]. The gas phase equations are

$$\frac{\partial(\rho u)}{\partial x} = 0 \tag{1}$$

$$\rho u \frac{\partial u}{\partial x} = -\frac{\mathrm{d}P}{\mathrm{d}x} + \frac{1}{r}\frac{\partial}{\partial r}\left(\mu r \frac{\partial u}{\partial r}\right) \tag{2}$$

$$\rho u \frac{\partial (c_p T_\mathrm{g})}{\partial x} - \frac{1}{r}\frac{\partial}{\partial r}\left(k_\mathrm{g} r \frac{\partial T_\mathrm{g}}{\partial r}\right) = 0 \tag{3}$$

$$\rho u \frac{\partial y_i}{\partial x} - \frac{1}{r}\frac{\partial}{\partial r}\left(\rho D_\mathrm{im} r \frac{\partial y_i}{\partial r}\right) = 0 \tag{4}$$

where r is the density of the gas mixture, k_g its conductivity, μ its viscosity and c_p its specific heat; $u(r,x)$ is the local velocity, a function of spatial coordinates, r and x; $T_\mathrm{g}(r,x)$ and $T_\mathrm{s}(x)$ are the gas phase and surface temperatures, respectively; y_i is the mass fraction of species i; D_im is its mixture diffusion coefficient. The contribution of the radial velocity component is neglected. The energy balance for the catalytic surface is

$$\rho_\mathrm{s} c_{p_\mathrm{s}} \varepsilon \frac{\partial T_\mathrm{s}}{\partial t} + k_\mathrm{s}\varepsilon \frac{\partial^2 T_\mathrm{s}}{\partial x^2} - k_\mathrm{g} \left.\frac{\partial T_\mathrm{g}}{\partial r}\right|_{r=a} = \dot{R}(-\Delta H) \tag{5}$$

where a is the radius of the cell, ρ_s the density of the substrate, k_s its conductivity, c_{p_s} its specific heat, and ε its half-thickness; $\dot{R}$ is the surface reaction rate with the heat of reaction, ΔH. Radiation heat transfer within the monolith passage is ignored because the influence of radiation heat transfer was minimized in the experimental design and plays a minor role in these physical and flow conditions.

The boundary conditions for these equations describe: the fluxes of each species at the catalyst surface (Eq. (6)); thermal continuity between the gas at the surface and the surface (Eq. (7)); zero flux of momentum, energy and species at the center of the cell; and adiabatic boundaries for the substrate at either end of the monolith. Also, it is assumed only axial conduction occurs within the cell wall, i.e., that radial heat flow is symmetric over a depth ε within the cell wall and no energy flows radially through the catalytic surface. The inlet gas phase temperature and concentrations are spatially uniform but may vary with time.

Table 1
Parameter values and conditions used in the calculations

Parameter	Value
Flow properties	
Inlet pressure	1 atm
Inlet gas temperature	400°C
Mean inlet flow velocity	7.59 m/s
Inlet C_3H_8 concentration	2.06 mol%
Inlet O_2 concentration	20.6 mol%
Mixture adiabatic flame temperature	1540°C
Inlet Reynolds number	186
Substrate properties	
Monolith cell diameter, $2a$	0.15 cm
Monolith cell density	200 cells/in.^{2}
Monolith wall thickness, 2ε	0.029 cm
Monolith length, L	1.96 cm
Wall density, ρ_s	1700 kg/m^3
Specific heat of wall, c_{p_s}	800 J/kg K
Wall thermal conductivity, k_s	1.4 W/m K
Pt loading, per weight of substrate	2 wt.%

$$-\rho D_\mathrm{im} \left.\frac{\partial y_i}{\partial r}\right|_{r=\mathrm{a}} = \dot{R}_i \tag{6}$$

$$T_\mathrm{g}|_{r=a} = T_\mathrm{s} \tag{7}$$

Physical parameters describing the monolith and the flow conditions used in the simulations are summarized in Table 1. The heterogeneous reaction kinetics are based on a first order global rate expression from [14] for propane oxidation on Pt, presented on the basis of monolith surface area, i.e., as an apparent reaction rate. The pre-exponential factor was modified assuming a linear relationship between catalyst activity and catalyst loading. The loading reported in the earlier study was 0.6 wt.% Pt and the loading here was 2.0 wt.%, so the pre-exponential factor was increased by a factor of 3.33.

$$\dot{R}_{\mathrm{C_3H_8}} = 1.039 \times 10^{11} \exp\left\{\frac{-17000}{RT}\right\} C_{\mathrm{C_3H_8}} \quad (\mathrm{mol\,cm^{-2}\,s^{-1}}) \tag{8}$$

It is assumed that propane is converted into CO_2 and H_2O only, i.e., neither intermediate species nor NO_x are considered [9,10].

The transient system of equations (1)–(5) are solved with a finite difference procedure described elsewhere [12]. The only change to the algorithm is inclusion of the continuity and momentum equations, Eqs. (1) and (2), respectively. The pressure gradient in the momentum equation (2) is adjusted until mass continuity across the cell ($\int \rho u r \, dr$) is maintained within a tolerance of 1×10^{-6}.

The solution to the temporally unmixed problem involves a time-varying fuel composition, modeled as a sinusoidal variation of specified amplitude and frequency. Consideration of the residence time within the cell and the period of the sinusoidal fuel variation is required to determine whether absence of transient terms in the gas phase equations (quasi-steady assumption) is too restrictive an approximation. For the quasi-steady assumption to hold, the period of the sinusoid must be larger than the residence time in the monolith cell, ideally much larger. The residence time within the catalyst is below 2.6 ms, while the shortest oscillation period in this study is 33 ms (30 Hz).

3.2. Homogeneous combustion model

Focus of the model for homogeneous combustion is placed on combustion chemistry, in particular on NO_x formation. Therefore, detailed chemistry must be included, whereas the flow system can be simplified by using a PFR [10].

The reaction mechanism for propane oxidation is taken from Warnatz [16] including data from the CEC evaluation group [17]. The NO mechanism originates from Bockhorn et al. [18], extended with $NO \leftrightarrow NO_2$ reactions from Miller and Bowman [19]. The complete reaction mechanism comprises 488 elementary reactions among 53 chemical species. This reaction mechanism is used as it is, i.e., without any adaptation to the measurements.

The outlet conditions of the catalyst model are used as inlet conditions to the PFR. It is assumed that radial temperature and concentration profiles emerging from the catalyst channel are immediately mixed at the inlet to the PFR (weight averaged concentration and temperature). PFR computations are performed for one full period of the "steady" periodic oscillation; i.e., at each point in time, a set of concentration and temperature was used as inlet to a PFR calculation. For purely homogeneous combustion (i.e., non-catalytic combustion) the PFR model was applied as well, but using the inlet conditions as for the catalyst model (i.e., inlet conditions to the combustion chamber at x=0 mm). In any case, it is assumed that the homogeneous combustion zone, defined as the maximum OH concentration, is located at the exit of the honeycomb monolith (x=20 mm). An "adaptive residence time" scheme is applied to account for fluctuations in residence time due to fluctuating inlet conditions. This is necessary because the suction probe used in the experiments is mounted at a fixed location at the exit of the combustion chamber (x=400 mm).

4. Results and discussion

4.1. Experimental data

Fig. 2 shows experimental data on NO_x emissions versus rms fuel fluctuations for both non-catalytic and catalytically stabilized lean premixed combustion. Data are shown for different fuel fluctuation frequencies of 10, 20, and 30 Hz. Note that certain rms values are achieved with different frequencies. NO_x emissions from catalytically stabilized combustion are

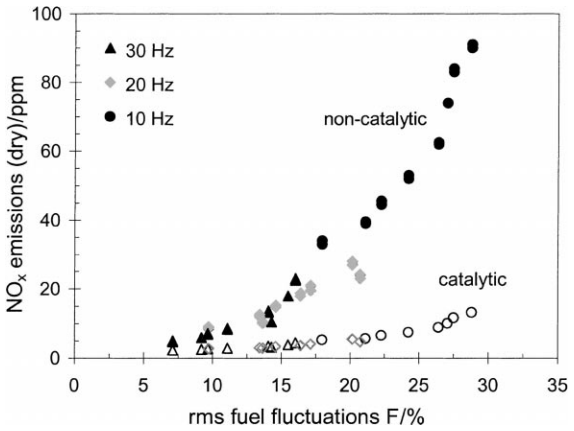

Fig. 2. Measured NO_x emissions at the combustion chamber exit (x=400 mm) versus rms fuel fluctuations for catalytically stabilized and non-catalytic combustion. Fuel flow pulse frequencies =10, 20 and 30 Hz, T_{in}=400°C, ϕ=0.5.

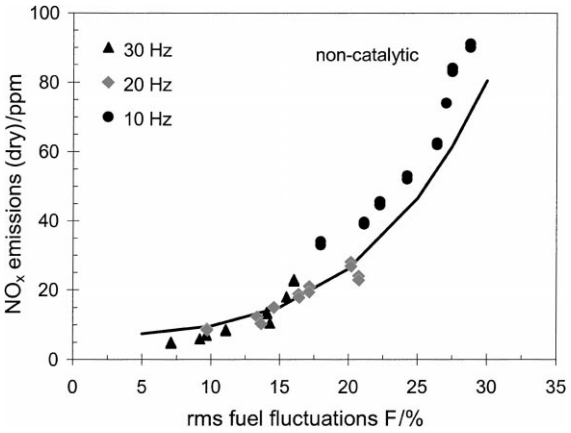

Fig. 3. Comparison of calculated NO_x emissions versus rms fuel fluctuations from non-catalytic combustion with experimental data. Symbols: measured at combustion chamber exit (x=400 mm), with different fuel pulse frequencies=10, 20 and 30 Hz, T_{in}=400°C, ϕ=0.5. Line: calculated NO_x emissions; the calculations do not depend on the fuel pulse frequency.

much less affected by increasing rms fluctuations than from non-catalytic combustion. Fig. 2 also indicates that NO_x emissions for both cases do not depend on the frequency but only on the rms.

4.2. Non-catalytic combustion

Fig. 3 shows a comparison with calculated NO_x emissions from non-catalytic combustion using the PFR code. NO_x emissions are derived by averaging NO_x emissions from the PFR calculations for one full period of fuel inlet fluctuations at a certain rms. There is only one curve for all different frequencies. This is because the fuel fluctuations, according to the experiments, are described as a sine-wave, i.e., computed NO_x emissions do not depend on the frequency, a finding that can be seen from Fig. 2 as well.

4.3. Catalytic model

The catalytic model shows, for all cases computed in this study, that the fuel conversion on the catalyst surface is diffusion-limited throughout the entire length of the catalyst, i.e., the catalyst lights-off at the inlet, transitioning immediately into the diffusion-limited regime. As a consequence, the mean fuel consumption is not significantly affected by the frequency nor the rms of the fuel fluctuations since the mean inlet conditions and the dimensions of the catalyst are the same. With the current settings, the mean fuel consumption is indeed found to be approximately 77% of the total fuel for all cases. These findings agree well with findings in other investigations, at least for the non-fluctuating (0% rms) cases. In [11] it has been shown, that catalytic propane conversion on platinum is indeed immediately diffusion-limited at inlet temperatures of 400°C and flow velocities of the same order of magnitude. In [4], the conversion has been estimated to be in the range 70–80% according to the measurements at non-fluctuating conditions. However, it is not clear yet, if this is true for fluctuating inlet conditions as well or if it is just a result of the surface kinetics chosen for this study (see modeling). Unfortunately, there is no data available on the fuel consumption within the catalyst at fluctuating conditions [4].

Fig. 4 shows propane mole fractions at the catalyst inlet and outlet for a case with 20 Hz and 20% rms fuel fluctuation versus time. Due to the fuel conversion within the catalyst the mean fuel concentration as well as the amplitude of the fluctuations are reduced. The rms fuel fluctuations $F = c'_{rms}/\bar{c}$, however, remain unchanged. This is to be expected, since the fuel conversion is diffusion-limited throughout the catalyst. However, the amount of fuel which is to be burnt

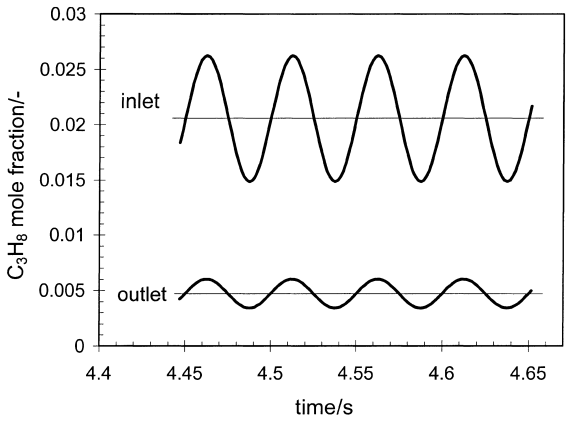

Fig. 4. Propane mole fractions at the inlet and outlet to the catalyst versus time for "stationary oscillating conditions". Inlet conditions: temporal fuel concentration fluctuations at the inlet to the catalyst, sine-wave in time with 20 Hz and 20% rms, T_{in}=400°C, ϕ=0.5.

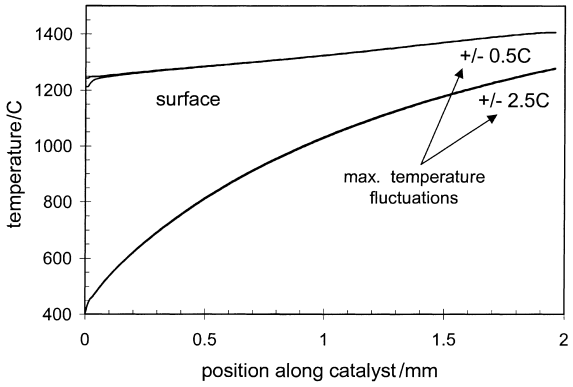

Fig. 5. Surface and bulk gas temperature profiles along the catalyst at maximum and minimum temperature excursions at stationary oscillating conditions. Inlet conditions: temporal fuel concentration fluctuations at the inlet to the catalyst, sine-wave in time with 20 Hz and 20% rms, T_{in}=400°C, ϕ=0.5. Temperature fluctuations are decreasing very quickly along the catalyst; maximum values are given for the exit region of the catalyst.

in the subsequent homogeneous combustion zone is substantially reduced.

Fig. 5 shows calculated surface and bulk gas temperature distributions along the catalyst for the 20 Hz/20% rms case at the most extreme conditions during one cycle of the inlet fluctuations. The temperatures are hardly affected in time. Only near the inlet, the surface temperature follows somewhat the fluctuations of the inlet conditions. This result demonstrates, that the thermal inertia of the catalyst acts as a very effective buffer for the fluctuating heat release on the surface, i.e., the extra heat released by a richer pocket passing through the catalyst is absorbed by the substrate and transferred to the following, leaner pocket. The resulting changes in surface temperature as well as in gas temperature are very small. As a result, the catalyst prevents the development of large temperature differences which would result in non-catalytic combustion, when burning rich and lean pockets alternately. It is these large temperature differences which cause overall higher NO_x emissions in non-catalytic combustion.

One could argue that this finding is a result of the 1D energy equation of the catalyst wall, i.e., the extra heat released on the surface is uniformly distributed into the catalyst wall with no temperature gradient across the wall. In order to justify the 1D simplification of the catalyst wall, the following considerations can be pursued.

Energy conservation requires that all energy fluxes to and from the surface are balanced at any time and surface node:

$$\dot{q}_{cond} = \dot{q}_{chem} + \dot{q}_{conv} \tag{9}$$

$\dot{q}_{chem}$ represents the chemical heat release due to fuel conversion on the surface (the fuel is transported in the gas phase) and $\dot{q}_{conv}$ is the heat transported to or from the surface via convective heat transfer in the gas phase. $\dot{q}_{cond}$ the conductive heat transfer within the wall, assuming that all net energy transported to or from the surface has to be conducted through the wall. Note that radiation is not included in the model (see catalyst model).

For the purpose of these considerations the term $\dot{q}_{cond}$ can be defined as

$$\dot{q}_{cond} = \frac{k_s \Delta T}{\varepsilon} \tag{10}$$

where k_s is the heat transfer coefficient of the wall material and ε the half-wall thickness. ΔT is the apparent temperature difference across the wall as the driving force for the heat transfer. Note that with a 1D formulation for the catalyst wall ΔT is neglected. With Eqs. (9) and (10) and $\dot{q}_{chem}$ and $\dot{q}_{conv}$ calculated from the numerical solutions of the 2D flow model, the apparent temperature difference ΔT can be derived for any position along the catalyst and varying times.

Fig. 6 shows apparent ΔT across the half-wall for the most extreme conditions during one full cycle of the fluctuations. The temperature differences are very small for most of the catalyst channel and reach somewhat significant values only at the very inlet. It can be concluded from Fig. 6 that a 1D formulation of the catalyst wall is admissible and does not constitute an oversimplification. This finding is important for future modeling purposes, since a 2D treatment of the catalyst wall is very costly in terms of computing time and can lead to severe problems with numerical convergence.

4.4. Hybrid catalytic model

Fig. 7 shows calculated gas temperatures and NO_x emissions versus time at the exit of the hybrid catalytic combustion chamber (x=400 mm) over one full cycle, again for the case with 20 Hz and 20% rms fuel

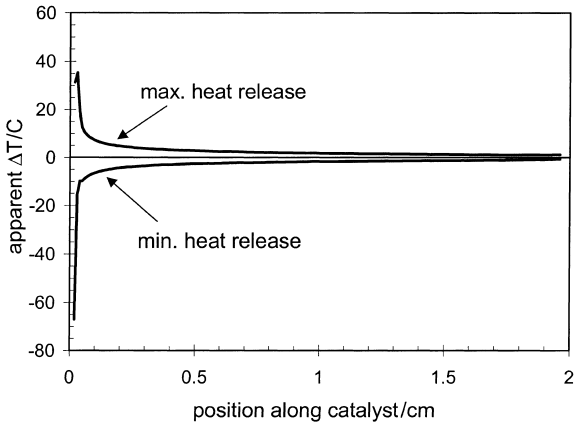

Fig. 6. Maximum and minimum profiles of apparent radial temperature difference ΔT_{rad} across the catalyst wall at stationary oscillating conditions. Inlet conditions: temporal fuel concentration fluctuations at the inlet to the catalyst, sine-wave in time with 20 Hz and 20% rms, T_{in}=400°C, ϕ=0.5.

fluctuations. The data shown is gained by coupling the catalyst model with the PFR model for the homogeneous combustion zone as described in the modeling section. Fig. 7 reveals that some temperature fluctuations (approximately +/−60 K) occur at the exit of the combustion chamber. These are caused by fuel fluctuations leaving the catalyst as shown in Fig. 4. As a consequence, NO_x concentrations as computed in the PFR fluctuate as well.

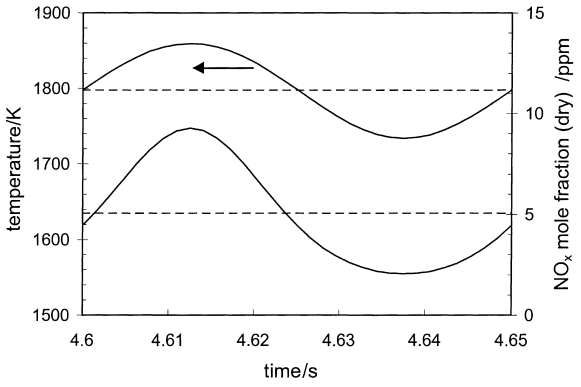

Fig. 7. Calculated gas temperatures and NO_x concentrations versus time at the exit of the hybrid catalytic combustion chamber (x=400 mm) over one full cycle of stationary oscillating conditions. Inlet conditions: temporal fuel concentration fluctuations at the inlet to the catalyst, sine-wave in time with 20 Hz and 20% rms, T_{in}=400°C, ϕ=0.5.

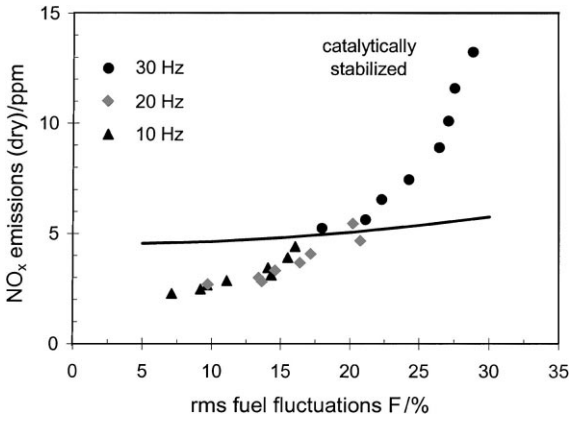

Fig. 8. Comparison of calculated NO_x emissions versus rms fuel fluctuations from hybrid catalytic combustion with experimental data. Symbols: measured at combustion chamber exit (x=400 mm), with different fuel pulse frequencies of 10, 20 and 30 Hz, T_{in}=400°C, ϕ=0.5. Line: calculated NO_x emissions for fuel pulse frequencies of 20 Hz; differences to 10 and 30 Hz are not significant.

Fig. 8 shows a comparison of measured and calculated NO_x emissions at the exit of the combustion chamber for different frequencies and rms fuel fluctuations. Calculated values are shown for one frequency only (20 Hz) as the differences to 10 and 30 Hz are negligible, a finding that is supported by the experiments as well. The agreement between experiments and modeling is not as good as with non-catalytic combustion. NO_x emissions are slightly over predicted at low rms and the trend for increasing NO_x emissions with increasing rms is much less pronounced. There is evidence in literature [9,11,18] that the reaction mechanism for propane used in this study somewhat over predicts prompt NO_x formation under these lean conditions, explaining the differences at low rms. However, it is not yet fully understood why the model under-predicts the trend with increasing rms. Given the good agreement between modeling and measurements in the non-catalytic case, one can assume that the discrepancy in the catalytically stabilized cases is caused mainly by the catalyst model and not the PFR model.

It is most likely that the catalyst model over predicts the fuel consumption, especially for greater rms fluctuations. Lower fuel consumption and/or larger fuel fluctuations at the exit of the catalyst model would cause increased NO_x emissions from the

homogeneous combustion zone. The catalyst model, as used in this study, assumes a one-step surface reaction for propane oxidation from literature [14]. With this assumption, the fuel conversion on the surface turns out to be diffusion-limited in any case, no matter how large the fluctuations are. This might not be the case in reality, i.e., dynamic effects in the surface and/or gas phase chemistry could play an important role, lowering the overall fuel consumption or increasing the magnitude of the concentration fluctuations. Future work will address these uncertainties with a more detailed reaction mechanism for the surface and gas phase in the catalyst model. This will also require a refinement of the experimental studies in order to determine the fuel consumption at the catalyst exit. This way the result from the catalyst model can be better validated.

5. Conclusion

Experimental data show that NO_x emissions from a hybrid catalytic combustor are much less increased with temporal fuel/air unmixedness than from a non-catalytic combustor. The catalyst model which is applied to investigate on the impact of the catalyst on the combustion process reveals the following main effects: (1) the catalyst lowers the mean fuel concentration and the magnitude of the fluctuations prior to the homogeneous combustion process downstream of the catalyst, (2) the catalyst's thermal inertia acts as a very effective buffer for the fluctuating heat release on the surface, i.e., extra heat released by a richer pocket passing through the catalyst is absorbed by the substrate and transferred to the following, leaner pocket, thereby preventing the development of large temperature fluctuations in the gas phase.

NO_x emissions from non-catalytic combustion can be modeled via a PFR with a detailed reaction mechanism including NO_x formation. This modeling approach shows very good agreement between experiments and calculations.

NO_x emissions from the hybrid catalytic combustor are studied numerically by coupling the catalyst model with a PFR, describing the homogeneous combustion process downstream of the catalyst, i.e., the outlet conditions of the catalyst model are used as inlet conditions to the PFR. The agreement between calculated and experimental NO_x emissions is not as good as with non-catalytic combustion, i.e., the model under-predicts the trend of increasing NO_x emissions with increasing rms fuel fluctuations. It is assumed that the one-step the catalyst surface chemistry from literature, as applied for the catalyst model, is predicting too high fuel consumption within the catalyst, so that NO_x formation in the subsequent homogeneous combustion zone is under-predicted. Future work needs to address these uncertainties with a more detailed reaction mechanism for the surface and gas phase in the catalyst model. This will also require a refinement of the experimental studies in order to determine the fuel consumption at the catalyst exit so that the catalyst model can be better validated.

Acknowledgements

The authors wish to thank Dr. A. Schlegel for his contributions to this work.

References

[1] T.F. Fric, AIAA Paper 92-3345, 1992.
[2] J.R. Maughan, R.E. Warren, A.K. Tobaldi, T.P. Roloff, ASME Paper No. 92-GT121, 1992.
[3] W.-P. Shih, J.G. Lee, D.A. Santavicca, Proceedings of the 26th International Symposium on Combustion, The Combustion Institute, Pittsburgh, PA, 1996, pp. 2771–2778.
[4] A. Schlegel, M. Streichsbier, R. Mongo, R.W. Dibble, ASME Paper No. 97-GT-306, 1997.
[5] W.C. Pfefferle, ASME Paper No. 75-WA/Fu-1, 1975.
[6] T. Furuya, S. Yamanaka, T. Hayata, J. Koezuka, T. Yoshine, A. Ohkoshi, ASME Paper No. 87-GT-99, 1987.
[7] V. Scherer, W. Weisenstein, T. Griffin, P. Benz, A. Schlegel, S. Buser, Proceedings of the Second International Conference on Combustion Technologies for a Clean Environment, Lisbon, Portugal, July 19–22, 1993.
[8] J.C. Schlatter, R.A. Dalla Betta, S.G. Nickolas, M.B. Cutrone, K.W. Beebe, T. Tsuchiya, ASME Paper No. 97-GT-57, 1997.
[9] A. Schlegel, S. Buser, P. Benz, H. Bockhorn, F. Mauss, Proceedings of the 25th International Symposium on Combustion, The Combustion Institute, Pittsburgh, PA, 1994, pp. 1019–1026.
[10] A. Schlegel, P. Benz, T. Griffin, W. Weisenstein, H. Bockhorn, F. Mauss, Combust. Flame 105 (1996) 332–340.
[11] A. Schlegel, Thesis, No. 10887, ETH Zürich, Switzerland, 1994.
[12] A.L. Boehman, J.W. Simons, S. Niksa, J.G. McCarty, Combust. Sci. Technol. 122 (1–6) (1997) 257–303.

[13] A.L. Boehman, J.W. Simons, S. Niksa, J.G. McCarty, J. Energy Res. Technol. 199 (3) (1997) 164–170.
[14] C. Bruno, P.M. Walsh, D.A. Santavicca, N. Sinha, Y. Yaw, Combust. Sci. Technol. 31 (1983) 43–74.
[15] R.J. Kee, J. Warnatz, J.A. Miller, Sandia Report SAND83-8209, 1983.
[16] J. Warnatz, in: W.C. Gardiner (Ed.), Combustion Chemistry, Springer, Berlin, 1984.
[17] D.L. Baulch, C.J. Cobos, R.A. Cox, C. Esser, P. Frank, Th. Just, J.A. Kerr, M.J. Pilling, J. Troe, R.W. Walker, J. Warnatz, J. Phys. Chem. Ref. Data 21/3 (1992) 411–734.
[18] H. Bockhorn, Ch. Chevalier, J. Warnatz, V. Weyrauch, ASME HTD, Vol. 166, Book No. G00629, 1991.
[19] J.A. Miller, C.T. Bowman, Progr. Energy Combust. Sci. 15 (1989) 287–338.